IET Generation, Transmission & Distribution

Research Article

IET Journals
The Institution of Engineering and Technology

Non-technical loss and power blackout detection under advanced metering infrastructure using a cooperative game based inference mechanism

ISSN 1751-8687
Received on 7th January 2015
Revised on 19th September 2015
Accepted on 22nd October 2015
doi: 10.1049/iet-gtd.2015.0003
www.ietdl.org

Tung-Sheng Zhan[1], Shi-Jaw Chen[2], Chih-Cheng Kao[1], Chao-Lin Kuo[3], Jian-Liung Chen[1], Chia-Hung Lin[1] ✉

[1]*Department of Electrical Engineering, Kao-Yuan University, Lu-Chu District, Kaohsiung City, 82151, Taiwan*
[2]*Department of Greenergy Science and Technology, Kao-Yuan University, Lu-Chu District, Kaohsiung City, 82151, Taiwan*
[3]*Department of Maritime Information and Technology, National Kaohsiung Marine University, Cijin District, Kaohsiung City, 80543, Taiwan*
✉ *E-mail: eechl53@gmail.com*

Abstract: To efficiently detect non-technical loss and power blackout in micro-distribution systems, this study proposes using a cooperative game (CG) based inference mechanism under the advanced metering infrastructure technique. Fractional-order Sprott system is designed to extract specific features between the profiled usages and the measurement usages in real time analysis. The fractional-order dynamic errors are positive correlated with the changes in load usages, including normal conditions, electricity fraudulent events, and power blackout events. Then, multiple agents in a game and multiple CG based inference mechanisms are used to locate abnormalities in micro-distribution systems. For energy management applications, the proposed inference mechanism can identify the 2.5–20% irregular usages during normal demand operations. In addition, it can also identify the large changes >20% in usages, while a micro-distribution system is disconnected to operate in the islanded mode within a few hours. This function can address an outage occurrence and then quickly resume service using the service restoration strategy and distributed generations in a local grid. Using a medium-scale micro-distribution system, computer simulations are conducted to show the effectiveness of the proposed inference model.

1 Introduction

Two main electricity distribution losses in a power system or in a distribution system include technical losses (TLs) and non-technical losses (NTLs) [1, 2]. Typical TLs are caused by the natural properties of the electrical components and depend on energy delivery through the transmission and distribution systems over long distances, such as winding and core losses in a transformer, transmission line or feeder losses, skin effect loss, and so on. These inherent losses can be measured and estimated, depending on the current in electric components. The NTLs occur as results of electricity fraud, metering, and recording errors, utility equipments, and embedded generation. Among those, large amounts of NTLs are absorbed by fraudulent electricity consumers. In addition, a power blackout is a transient power failure or a long-term power loss in a local zone. These events include electrical equipment faults, transmission line damage, short circuit faults, or overloading. The profile differences of overall events are shown in Fig. 1.

For energy management situations, power utilities can handle metering data of customers' energy consumption with the metering, monitoring, and billing systems [3, 4]. In practical measurements, meter reading requires routine validation, and readings within 50 and 200% of the expected value [5] are regarded as acceptable levels to separate irregular power customers and chastity customers. In terms of current technological support, an advanced meter infrastructure (AMI) has the automated and bidirectional architecture between smart utility meters and a utility company [6–8]. Remote meter data are received by the AMI host system and sent to the meter data management (MDM) system for further analysis and data storage. This is to allow utility companies to monitor the real-time data of power consumption, operation status, and billing purposes. Therefore, an AMI can provide support in detecting NTLs and addressing blackout events.

Fraudulent consumption involves one or more consumers that act secretly to avoid billing charge. A blackout is the most severe event and total power is lost. After a fault clearing, energy service restoration and distributed generations (DGs), such as solar/wind generation systems, micro-generator, and diesel-generator, are employed to quickly recover overall or partial loads. Both of them relate to the duration and effect of the usage from a few hours to a few days. To detect the abovementioned unwanted events, statistical and artificial intelligent (AI) techniques, or combining those [1, 2, 8–14] have offered promising solutions in a power system or in a distribution system. Based on statistical techniques, load patterns are regarded as periodic or non-periodic signals in the time domain, which could indicate gradual changes in time and amplitude for regular usages. When electricity fraudulent events occur, the load patterns will produce violent power changes in frequencies and amplitudes for irregular usages, as seen in Fig. 1. The power interruption and severe amplitude drops occur for long-term or short-term blackouts. For time-frequency analysis, previous studies [11] proposed fast Fourier transform, short time Fourier transform, or discrete wavelet transform to detect frequency spectral changes. However, these methods need to assign greater resolution in time with cascaded low-pass or high-pass filters and down-sampling/up-sampling operations to process board ranges of frequency bands. For time-varying, random, and irregular signal analysis, it is difficult to choose the size of the sampling window, due to frequent events and transient events. However, these methods require a large knowledge database and consider various electricity theft behaviours, such as bypassing, resetting, and tampering meters or introducing unwanted harmonics [15]. Then AI methods, such as artificial neural networks (ANNs) [1, 10], support vector machines (SVMs), SVM with genetic algorithm, Fuzzy inference systems [2, 11, 12], and game theory [4, 8, 14], combine signal processing and feature

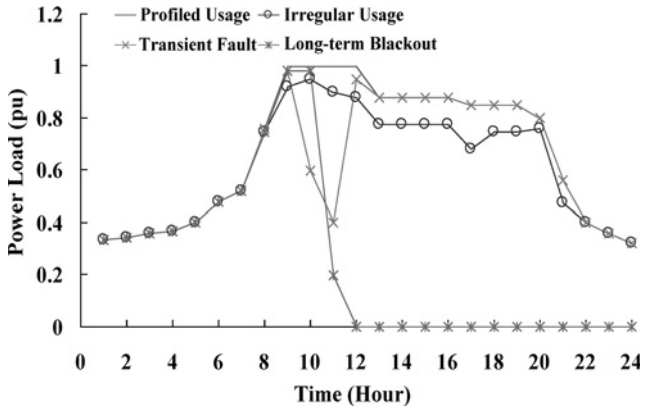

Fig. 1 *Profile differences for regular usage, irregular usage, and power blackout*

extraction methods to identify customers with irregular and fraudulent consumption.

To analyse irregular load patterns in the time domain, the Sprott system [16–19] is used to construct a quantifiable model for extracting self-synchronisation errors between the profiled usages and the measurements usages. A Sprott, consisting of a master system (MS) and a slave system (SS) [18, 19], has a coupling variable to extract differences between each other. The fractional-order formulation is used to find the dynamic errors related to the changes in load usages [8], and linear mapping shows a positive correlation as fractional-order dynamic errors (FODEs) gradually increase, involving fraudulent consumption events and blackout events. In terms of the evolutionary FODEs from normal condition to fraudulent consumption or normal condition to power blackout, evolutions might be a combination of the decreased probability of the normal conditions and the increased probability of abnormal conditions. In a game model, if there are changes in the FODEs, each event against each event is against and does not compromise. Then, based on the quantification analysis, the problem of abnormalities detection can be formulated as a cooperative game (CG) with multi-agents. The CGs can be utilised to design an inference mechanism with general probability formulations [20, 21], and can be integrated multi-agents under the AMI. This inference model has the ability to extract time-varying signals with violent changes, and parameter-less CGs do not require an objective function, parameters, and do not compute iteratively to achieve the optimal solutions.

In this study, we address the AMI to attempt to monitor energy usage data, including each customer's load profile and voltages, and validate the viability of the CG based inference mechanism by performing penetration testing on a small-scale micro-distribution system. The rest of this paper is organised as follows: Section 2 addresses the measurement support under AMI. Section 3 describes the CG-based inference mechanism for NTL detection. In Sections 4 and 5, simulation results, discussion, and a conclusion are given to show the efficiency of the proposed models.

2 Metering support under AMI

A digital smart meter is an energy meter that can measure electricity consumers' energy consumption, switch status, operational conditions, and billing charges, and also securely communicate those to the power utilities, as shown in Fig. 2. Bi-directional communication provides information collection and feeds back control commands to a main grid or a local distribution grid. This structure is called a 'micro-distribution system' which consists of radial feeders, renewable energy sources, storage devices, and local loads. Smart meters/intelligent meters can be used to monitor and control electricity devices at the customer's premises. For the load and bill management situation, power utilities use data concentrators to monitor customers' load demands and operational conditions.

Moreover, an AMI provides a metering technique to replace the analogue meters. Intelligent/smart electric meters (I/SEMs) are used to gather important information about voltage, current, power, outages, and so on using power line communications and wireless mesh topologies [22–24]. These two components can limit the maximum consumption, and disconnect and restore the electricity supply when a fault occurs or clears. In a smart grid environment, metering data from each consumer at regular time intervals allows a power utility to efficiently manage electricity demand. Each smart meter has a unique identifier and timestamp,

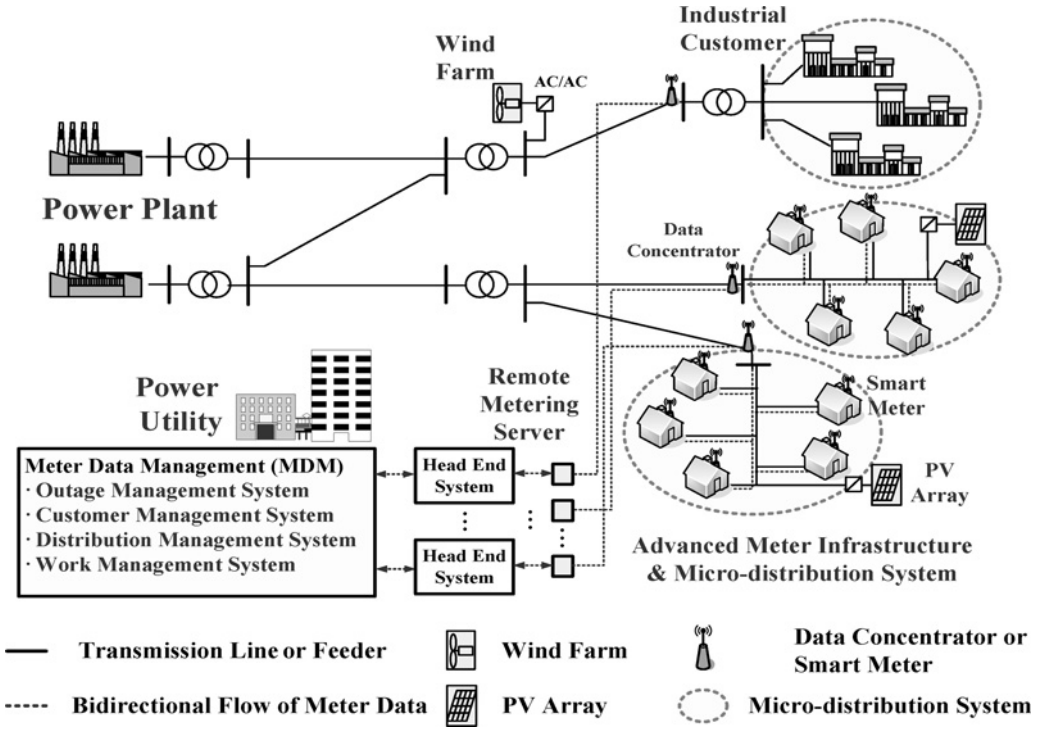

Fig. 2 *Schematic diagram of an AMI and micro-distribution system*

IET Gener. Transm. Distrib., 2016, Vol. 10, Iss. 4, pp. 873–882

thus overall instantaneous measured and commanded data can ensure bi-directional communications. In summary, an AMI offers the following functions [7, 25]:

- monitor and record the usage of load profiles,
- detect outages and verify online restoration,
- deliver and receive commanded messages for controlling smart appliances and disconnect remote switches in homes and buildings,
- detect the illegal abstraction of electricity equipment or service without a billing charge.

Thus, customers' historical consumption patterns, including regular usages, possible irregular usages, transient power blackout, and long-term power blackout can be faithfully recorded under real time conditions. AMI can provide available information for customers or distribution system operators, such as real power, outages, and billing charges, using the bidirectional communications between the main grid and the local grids. Then, through combining a feature extraction method and a detector, it is possible to identify illegal consumption in micro-distribution systems. In addition, an outage event can be addressed in any local distribution grid. After a fault is detected and a faulted section is isolated, un-faulted zones can also be energised by the local DGs (islanded mode), or be recovered to the main grid (grid-tie mode) by the service restoration strategy. Therefore, an AMI or an advanced grid infrastructure (AGI) [7, 26] can provide support for NTLs and power blackout detection.

3 Implementation of a CG based inference mechanism

3.1 NTL and blackout events' definition

In Taiwan, fraudulent activities cause 1.5–10% changes in local load usages and the average is 2.5% of total electricity loss. Illegal consumption costs an estimated 0.5 billion Taiwan dollars every year. For morphology analysis, typical fraudulent activities have changes in load usage as

$$\Delta P_r(t) = \left(\frac{P_{r,\mathrm{pro}}(t) - P_{r,\mathrm{mea}}(t)}{P_{r,\max}} \right) \tag{1}$$

where $\Delta P_r(t)$ is per-unit (pu) quantity for per hour or per quarter hour, $P_{r,\mathrm{pro}}(t)$ is the total profiled usage in the rth electricity consumer, $r = 1, 2, 3, \ldots, N_r$, $P_{r,\mathrm{mea}}(t)$ is the real-time measurement usage, and $P_{r,\max}$ is the maximum value of profiled usage.

Given the overload, normal condition, fraud and power blackout events, the changes in load usages have the following conditions [8]:

- overload: $\Delta P_r(t) < -0.025$ for overload,
- normal condition: $-0.025 < \Delta P_r(t) < +0.025$ for no violent changes,
- fraudulent activities: $+0.025 \le \Delta P_r(t) < +0.050$ for likely fraud events (average changes 2.5% in Taiwan), $+0.050 < \Delta P_r(t) < +0.200$ for serious fraud events,
- blackout events: $\Delta P_r \ge +0.200$ for faulted devices / loads clearing with a long-term power loss.

3.2 Feature extraction method

For quantitating the differences between regular and irregular usages, chaos synchronisation systems based detectors, such as Lorenz, Chen-Lee, and Sprott systems [16–19], are used to detect disturbances, irregularity and transit signals or patterns. Among these, the Sprott system is a simple model and a linearised system describing the dynamic evolution of the differences between coupled chaotic systems, as shown in Fig. 3. To design a feature extraction method, suppose two identical chaotic systems, $\dot{y}_{\mathrm{m}}$ and $\dot{x}_{\mathrm{s}}$, are coupled as a master (m) system and a slave (s) system [16]

$$\begin{bmatrix} \dot{y}_{1\mathrm{m}} \\ \dot{y}_{2\mathrm{m}} \\ \dot{y}_{3\mathrm{m}} \end{bmatrix} = \begin{bmatrix} 0 & 1 & 0 \\ 0 & 0 & 1 \\ -1.2 & -b & -a \end{bmatrix} \begin{bmatrix} y_{1\mathrm{m}} \\ y_{2\mathrm{m}} \\ y_{3\mathrm{m}} \end{bmatrix} + \begin{bmatrix} 0 \\ 0 \\ 2\,\mathrm{sign}(y_{1\mathrm{m}}) \end{bmatrix},$$
$$\mathrm{sign}(y_{1\mathrm{m}}) = \begin{cases} +1, & \text{if } y_{1\mathrm{m}} \ge 0 \\ -1, & \text{if } y_{1\mathrm{m}} < 0 \end{cases} \tag{2}$$

$$\begin{bmatrix} \dot{x}_{1\mathrm{s}} \\ \dot{x}_{2\mathrm{s}} \\ \dot{x}_{3\mathrm{s}} \end{bmatrix} = \begin{bmatrix} 0 & 1 & 0 \\ 0 & 0 & 1 \\ -1.2 & -b & -a \end{bmatrix} \begin{bmatrix} x_{1\mathrm{s}} \\ x_{2\mathrm{s}} \\ x_{3\mathrm{s}} \end{bmatrix} + \begin{bmatrix} 0 \\ 0 \\ 2\,\mathrm{sign}(x_{1\mathrm{s}}) \end{bmatrix},$$
$$\mathrm{sign}(x_{1\mathrm{s}}) = \begin{cases} +1, & \text{if } x_{1\mathrm{s}} \ge 0 \\ -1, & \text{if } x_{1\mathrm{s}} < 0 \end{cases} \tag{3}$$

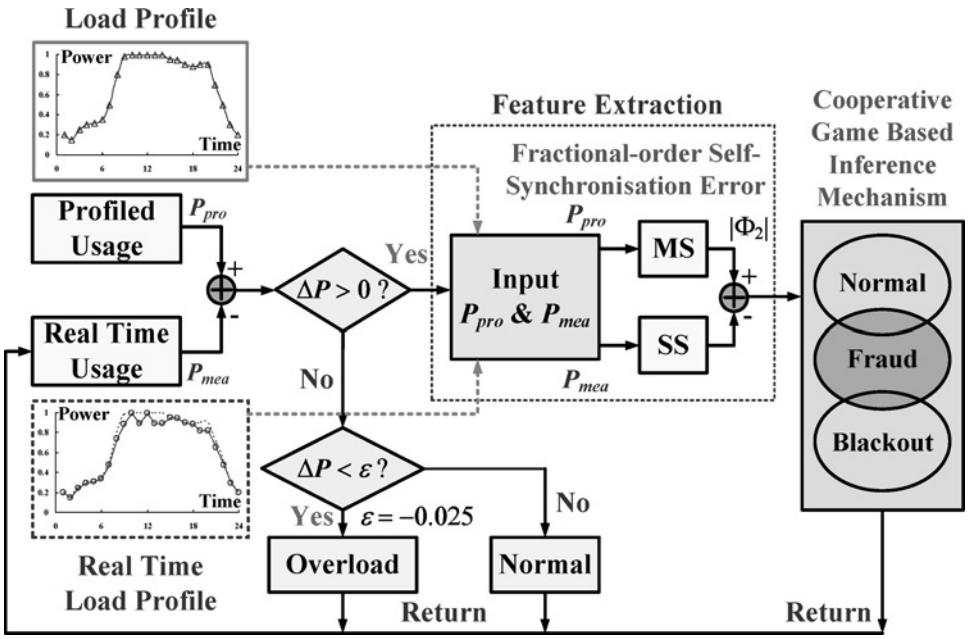

Fig. 3 *Diagram of proposed feature extraction and CG based inference mechanism*

where a Sprott system consisting of a 'MS' as a reference and a 'SS', as seen in Fig. 3, are denoted by subscripts 'm' and 's', respectively, and sign(y_{1m}) and sign(x_{1s}) are the signum functions. Variables, y_{1m} and x_{1s}, are always positive for denoting the profiled usages and measurement usages in this study, hence the term, $2[\text{sign}(y_{1m}) - \text{sign}(x_{1s})] = 0$. Thus, systems (2) and (3) can be presented by differential equations, $\dot{Y}_m = AY_m$ and $\dot{X}_s = AX_s$, $Y_m = [y_{1m}, y_{2m}, y_{3m}]^T$, $Y_m \in R^3$, $X_s = [x_{1s}, x_{2s}, x_{3s}]^T$, $X_s \in R^3$.

To extract dynamic errors, the variables are defined as $e_1 = (y_{1m} - x_{1s})$, $e_2 = (y_{2m} - x_{2s})$, and $e_3 = (y_{3m} - x_{3s})$, and $e = [e_1, e_2, e_3]^T$. By subtracting (3) from (2), the error system can be expressed by

$$\begin{bmatrix} \dot{e}_1 \\ \dot{e}_2 \\ \dot{e}_3 \end{bmatrix} = \begin{bmatrix} 0 & 1 & 0 \\ 0 & 0 & 1 \\ -1.2 & -b & -a \end{bmatrix} \begin{bmatrix} e_1 \\ e_2 \\ e_3 \end{bmatrix} \tag{4}$$

The differential equations, $\dot{e}_2$ and $\dot{e}_3$, form a linear system decoupled from the variable e_1, with the form

$$\begin{bmatrix} \dot{e}_2 \\ \dot{e}_3 \end{bmatrix} = \begin{bmatrix} 0 & 1 \\ -b & -a \end{bmatrix} \begin{bmatrix} e_2 \\ e_3 \end{bmatrix} = [A]\tilde{e} \tag{5}$$

subject to system parameters, $a > 0$ and $b > 0$ [18, 19].

According to the Grünwald–Letnikov fractional approximation [18], a general fractional-order differentiation formulation can be expressed as

$$\frac{\mathrm{d}^\alpha e(t)}{\mathrm{d}t^\alpha} = \lim_{\Delta t \to 0} \frac{e(t) - \alpha e(t - t_0)}{(t - (t - t_0))^\alpha} \simeq \frac{e(t) - \alpha e(t - t_0)}{(t_0)^\alpha} \tag{6}$$

The fractional derivative of a function depends on all of its past values. If the parameter α is taken to be 1, then the rate of change is the slope, and for the range 0 to1, (6) defines the fractional rate of change of the function $e(t)$.

To express the fractional-order differential system, the first-order differential system (5) is modified with fractional-order derivatives, as follows

$$\begin{bmatrix} D_t^\alpha e_2 \\ D_t^\alpha e_3 \end{bmatrix} \simeq \begin{bmatrix} 0 & t' \\ -b' & -a' \end{bmatrix} \begin{bmatrix} e_2(t) \\ e_3(t) \end{bmatrix} + \begin{bmatrix} 0 & -\alpha t' \\ -\alpha b' & -\alpha a' \end{bmatrix} \times \begin{bmatrix} e_2(t - t_0) \\ e_3(t - t_0) \end{bmatrix} \tag{7}$$

$$t' = \frac{1}{(t_0)^\alpha}, \quad a' = \frac{a}{(t_0)^\alpha}, \quad b' = \frac{b}{(t_0)^\alpha} \tag{8}$$

where the $(t - t_0)$ and t points are geometric approximations of the αth derivative, and t_0 is the time interval. The parameter, α, is the fractional order, with satisfying, $0 < \alpha < 1$, which is the first-order derivative definition, when the $\alpha = 1$ is the first-order derivative.

In this study, a fractional-order self-synchronisation error system, is used to extract various FODEs' between profiled usage, P_{pro}, by obtaining via load prediction (at least 1 week), and measurement usage, P_{mea}, as shown in Fig. 4. Suppose the discrete variables, $y_{2m} = P_{pro}[n]$ and $y_{3m} = P_{pro}[n + 1]$, $n \in [1, N - 1]$, are a data sequence obtained from the profiled usages. This sequence is stored in memory. The discrete variables, $x_{2s} = P_{mea}[n]$ and $x_{3s} = P_{mea}[n + 1]$, are a data sequence obtained from the real time measurement usage, which are stored hour-by-hour or quarter hour-by-quarter hour in the register for on-line application. Hence, the time interval, t_0, is the number of sampling points, N, in one day, $N = 24$ of per hour and $N = 96$ for per quarter hour, as shown in Fig. 4*a*. Therefore, the system (7) can be modified as a discrete

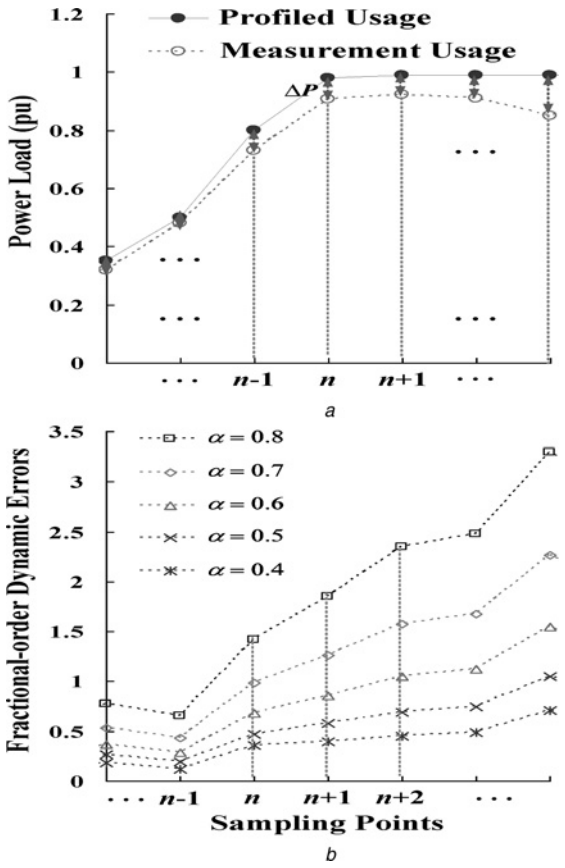

Fig. 4 *Fractional-order self-synchronisation error system, is used to extract various FODEs*

a Power load against sampling point,
b FODEs against sampling point

fractional-order error system

$$\begin{bmatrix} \Phi_1[n] \\ \Phi_2[n] \end{bmatrix} \simeq \begin{bmatrix} 0 & t' \\ -b' & -a' \end{bmatrix} \begin{bmatrix} e_2[n] \\ e_3[n] \end{bmatrix} + \begin{bmatrix} 0 & -\alpha t' \\ -\alpha b' & -\alpha a' \end{bmatrix} \times \begin{bmatrix} e_2[n - 1] \\ e_3[n - 1] \end{bmatrix}, \quad n \in [1, N - 1] \tag{9}$$

where the error variables are $e_2[n] = P_{pro}[n] - P_{mea}[n] = \Delta P[n]$, $e_3[n] = P_{pro}[n + 1] - P_{mea}[n + 1] = \Delta P[n + 1]$, $e_2[n - 1] = P_{pro}[n - 1] - P_{mea}[n - 1] = \Delta P[n - 1]$, $e_3[n - 1] = P_{pro}[n] - P_{mea}[n] = \Delta P[n]$, and the initial conditions are $P_{pro}[0] = P_{mea}[0] = 0$. The discrete formulations, Φ_1 and Φ_2, as detectors, can be used to extract the FODEs. The fractional-order dynamic error, $|\Phi_2(\Delta P)|$, is calculated using (10), as [8]

$$|\Phi_2(\Delta P)| = |-b'\Delta P[n] - a'\Delta P[n + 1] - \alpha b'\Delta P[n - 1] - \alpha a'\Delta P[n]| \tag{10}$$

where the system parameters, $a = 1$ and $b = 0.5$ in this study, and time interval, $t_0 = (24/N)$, required per hour for data sampling. Fig. 4*b* shows the FODEs with $\alpha = 0.80$–0.4. Equation (10) is used to extract the specific features between the profiled usage and the measurement usages.

3.3. CG model

Game theory can be divided into two models, a CG [20, 21] and non-CG [14, 27]. A CG consists of a set of agents and characteristic functions specifying the strategies created by the agents in a game. The cooperation behaviours allow a probability function to be

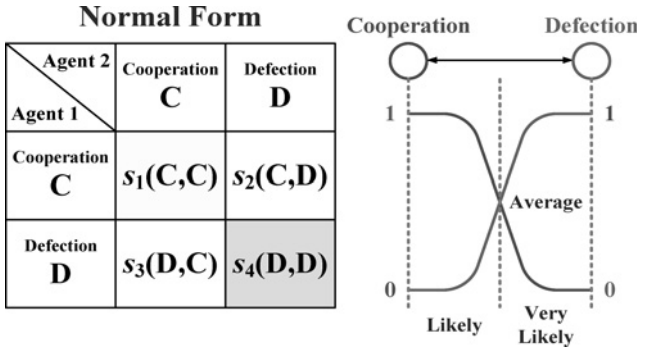

Fig. 5 *Normal form of a CG and its evolutionary dynamics of strategies*

assigned to each strategy, such as with the Bayesian rule and statistical decision functions [28, 29]. It also allows support decision-making applications, wherein at least two agents or several agents simultaneously make their strategies. Let two agents, a normal form of a game can be represented by a matrix or a table that shows the agents, strategies, and payoffs, as shown in Fig. 5.

As seen in normal form, each agent can choose either cooperation (C) or defection (D). The strategy combination of a game is s_1(C, C), s_2(C, D), s_3(D, C), and s_4(D, D). These strategies have evolutionary dynamics from cooperation (C) to defection (D), as shown in Fig. 5. According to Prisoner's dilemma game [20], a game can express the cooperative behaviours: (i) reward payoff for both agents cooperating; (ii) sucker's payoff or temptation payoff for one agent cooperating and another agent defecting; (iii) punishment payoff for both agents defecting. Therefore, the cooperation and defection behaviours have inverse payoffs. It can be assumed each strategy is a probability function between '0' and '1', as shown in Fig. 5. For a CG based inference mechanism, we have three inequalities for evolutionary dynamics [21]:

- reward stage (cooperation): $s_2(\mathrm{C, D}) > s_4(\mathrm{D, D})$ or $s_1(\mathrm{C, C}) > s_3(\mathrm{D, C})$
- sucker and temptation stage: $s_1(\mathrm{C, C}) + s_2(\mathrm{C, D}) > s_3(\mathrm{D, C}) + s_4(\mathrm{D, D})$,
- punishment stage (defection): $s_1(\mathrm{C, C}) + (2 \times s_2(\mathrm{C, D})) < s_3(\mathrm{D, C}) + (2 \times s_4(\mathrm{D, D}))$.

3.4 Implementation of CG based inference mechanism

We have a total of 110 simulation data, including 40 for normal conditions (N), 35 for fraud event (F), and 35 for blackout event (B). Fig. 6*a* shows the changes in load usages against FODEs, $|\Phi_2(\Delta P)|$, with the fractional order $\alpha = 0.80$. Referring to $0.000 \leq \Delta P < 0.025$, the FODE, $0.000 < |\Phi_2| < 1.9185$ is defined as the specific range for normal conditions, as $0.025 < \Delta P < 0.200$, the FODE, $1.9185 < |\Phi_2| < 5.4099$ is defined for fraud events, and $|\Phi_2| > 5.4099$ for detecting blackout events. The related parameters for the three events are shown in Table 1. Depending on the values of the certainty factors (CFs) against the changes in load usages, the FODEs gradually increase from normal conditions to blackout events. The follow-up evolutions can express three probability functions, as shown in Fig. 6*b*, and can be represented as $N(\Phi_2(\Delta P))$, $F(\Phi_2(\Delta P))$, and $B(\Phi_2(\Delta P))$

$$N(\Phi_2(\Delta P)) = \begin{cases} 1, & 0 \leq \Delta P < 0.025 \\ \exp\left(-1 \times \left(\dfrac{\Phi_2 - \Phi_{21}}{\sigma_1}\right)^2\right), & 0.025 \leq \Delta P < 1 \end{cases} \tag{11}$$

$$F(\Phi_2(\Delta P)) = \exp\left(-1 \times \left(\frac{\Phi_2 - \Phi_{22}}{\sigma_2}\right)^2\right), \quad 0 \leq \Delta P \leq 1 \tag{12}$$

$$B(\Phi_2(\Delta P)) = \begin{cases} \exp\left(-1 \times \left(\dfrac{\Phi_2 - \Phi_{23}}{\sigma_3}\right)^2\right), & 0 \leq \Delta P < 0.200 \\ 1, & 0.200 \leq \Delta P \leq 1 \end{cases} \tag{13}$$

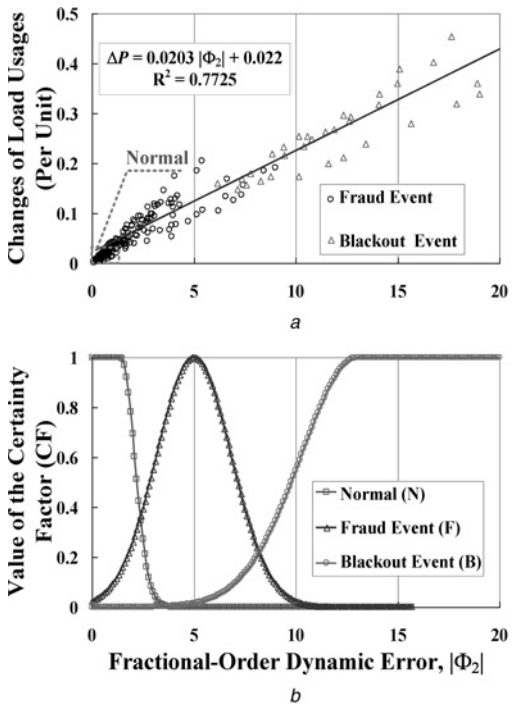

Follow-up / Baseline	Fraud F`	Fraud F	Blackout B`	Blackout B
Normal N	s_1(N,F`)	s_2(N,F)	s_5(N,B`)	s_6(N,B)
Normal N`	s_3(N`,F`)	s_4(N`,F)	s_7(N`,B`)	s_8(N`,B)
Fraud F	Null	Null	s_9(F,B`)	s_{10}(F,B)
Fraud F`	Null	Null	s_{11}(F`,B`)	s_{12}(F`,B)

c

Fig. 6 *Changes in load usages against FODEs*

a Changes in load usages against FODEs
b Values of CFs against the FODES
c Extensive form game

Table 1 Related parameters for the three events

Parameter	Event		
	Normal (40)	Fraud (35)	Blackout (35)
range of ΔP	0.000–0.025	0.025–0.200	>0.200
mean of FODE	$\Phi_{21} = 0.9357$	$\Phi_{22} = 5.0008$	$\Phi_{23} = 13.0621$
standard deviation	$\sigma_1 = +0.4545$	$\sigma_2 = \pm 2.5924$	$\sigma_3 = -3.9325$

where Φ_{21}, Φ_{22}, and Φ_{23} are the mean values of FODE, σ_1, σ_2, and σ_3 are the standard deviations, as shown in Table 1. The FODEs divided into three specific ranges from normal conditions to blackout events. Initially, one against one compromises or cooperates, the so-called 'reward stage'. Two events are against and do not compromise, while the FODE gradually increases, the so-called 'sucker and temptation stage' to 'punishment stage'. For multiple agents in a game, (11) to (13) are defined as agents' strategies, and their conflicting strategies are $N' = 1 - N(\Phi_2(\Delta P))$, $F' = 1 - F(\Phi_2(\Delta P))$, and $B' = 1 - B(\Phi_2(\Delta P))$. In this study, suppose each electricity consumer is willing to bill and keep micro-distribution's safety. Each pair of event are in conflict, and $N(\Phi_2(\Delta P))$, $F(\Phi_2(\Delta P))$, and $B(\Phi_2(\Delta P))$ are independent. Overall evolutionary dynamics of three events can be expressed an extensive form game and rational outcomes to make decisions, as shown in Fig. 6*c*. Three events are independent if and only if their joint probabilities are 'multiplication rule'. We have the following two CGs for each electricity consumer, $r = 1, 2, 3, \ldots, N_r$:

- Game I: normal condition (defined as C) changes to fraud events (defined as D) or to blackout event (D). The normal form is given by (see (14))

where the payoffs, s_1 and s_5, are relevant combinations for normal conditions, satisfying with inequalities: $s_2 > s_4$ and $s_5 > s_7$; the payoff, s_4, for fraud event, satisfying with an inequality: $s_1 + (2 \times s_2) < s_3 + (2 \times s_4)$; and the payoff, s_8, for blackout event, satisfying with an inequality: $s_5 + (2 \times s_6) < s_7 + (2 \times s_8)$. When $s_2 = s_4$ and $s_1 + (2 \times s_2) = s_3 + (2 \times s_4)$, Φ_1* is the first equilibrium point; $s_5 = s_7$ and $s_5 + (2 \times s_6) = s_7 + (2 \times s_8)$, Φ_2* is the second equilibrium point.
- Game II: fraud event changes (defined as C) to blackout event (defined as D). The normal form is given by

$$S_r^{II} = \begin{bmatrix} s_9(F \cap B') & s_{10}(F \cap B) \\ s_{11}(F' \cap B') & s_{12}(F' \cap B) \end{bmatrix} = \begin{bmatrix} F \times (1-B) & F \times B \\ (1-F) \times (1-B) & (1-F) \times B \end{bmatrix} \quad (15)$$

where the payoff, s_9, is a relevant combination for fraud event, satisfying with an inequality: $s_{10} > s_{12}$; and the pay-off, s_{12}, for blackout event, satisfying with an inequality: $s_9 + (2 \times s_{10}) < s_{11} + (2 \times s_{12})$. When $s_{10} = s_{12}$ and $s_9 + (2 \times s_{10}) = s_{11} + (2 \times s_{12})$, Φ_3* is the second equilibrium point.

In NTL and power blackout detection, logic inference with 'maximum composite operations' is used to generate the possible result, S^+ as

$$S_{\mathrm{m}}^{+} = \max_{0 \le \Phi_2 \le \Phi_{\max}} [\max[\max(s_1, s_4),\ \max(s_5, s_8)],\ \max(s_9, s_{12})]$$

$$\Phi_{\max} = \frac{(\Delta P_{\max} - 0.022)}{0.0203} \quad (16)$$

where $\Delta P_{\max}$ is the maximum change in load usage; $m = 1$, 2, and 3, $m = 1$ for the normal condition (N), $m = 2$ for fraud event (F), and $m = 3$ for blackout event (B). In addition, a joint payoff is used to detect any premonitory disturbance, as

$$S^{-} = S_1[s_1] \times S_2[s_1] \times \cdots \times S_r[s_1] \times \cdots S_{N_r}[s_1] \quad (17)$$

where N_r is the number of electricity consumers, $r = 1, 2, 3, \ldots, N_r$; S^- is an index, its value is less than 0.5, meaning a serious F event or a B event occurrence in a local micro-distribution system.

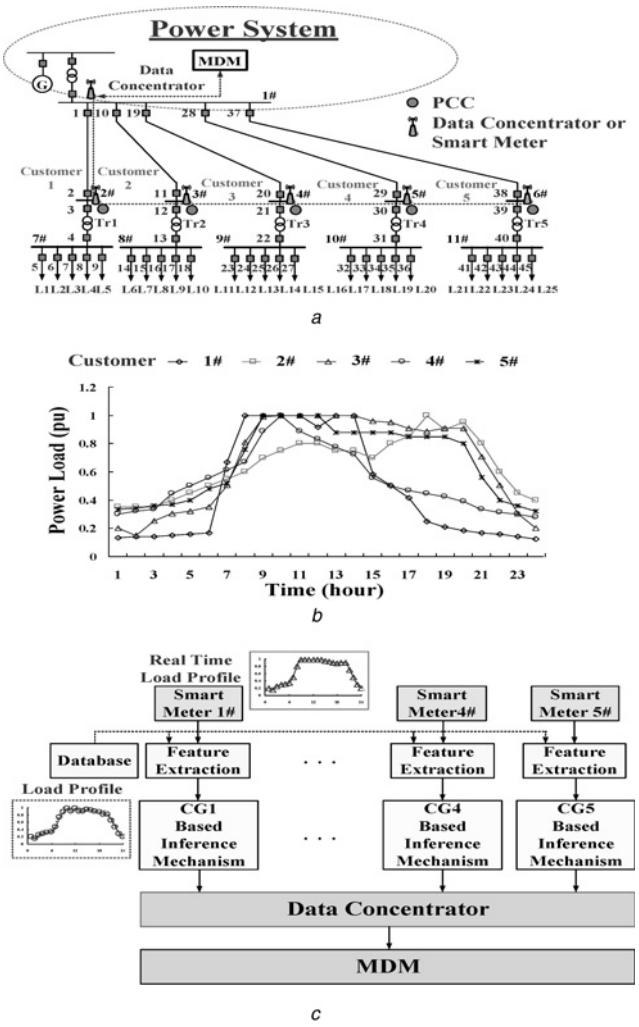

Fig. 7 *Medium-scale micro-distribution system is used as a case study*
a Structure of a medium-scale micro-distribution system
b Load patterns in per unit for five electricity customers
c Structure of CG based inference mechanism under AMI

4 Simulation results and discussion

A medium-scale micro-distribution system is used as a case study, as shown in Fig. 7*a*. The micro-distribution system consists of five customers), five transformers (138 kV/13.8 kV, 12MW), and 25 loads. The daily load patterns are shown in Fig. 7*b*. Overall data are practical measurements in per-unit per hour. Under the AMI, power utilities can monitor and store electricity customers' daily load usages in a micro-distribution system. We assume each smart meter can act correctly. It provides bi-directional communications between the smart meter and MDM, facilitating information awareness at the point of common coupling (PCC). The proposed

$$S_r^{I} = \begin{bmatrix} s_1(N \cap F') & s_2(N \cap F) & s_5(N \cap B') & s_6(N \cap B) \\ s_3(N' \cap F') & s_4(N' \cap F) & s_7(N' \cap B') & s_8(N' \cap B) \end{bmatrix} = \begin{bmatrix} N \times (1-F) & N \times F & N \times (1-B) & N \times B \\ (1-N) \times (1-F) & (1-N) \times F & (1-N) \times (1-B) & (1-N) \times B \end{bmatrix} \quad (14)$$

feature extraction method and CG based inference mechanism are employed to detect NTLs and power blackout events. Then, MDM can perform validation and identify the location where an abnormal event occurs. In this study, the FODEs, $|\Phi_2(\Delta P)|$, were calculated using (10) with $\alpha = 0.8$, with the system parameters $a = 1 > 0$, $b = 0.5 > 0$ [8, 18], and needed per hour for data sampling. The proposed multiple CG based inference mechanisms were developed on a personal computer (PC) AMD Athlon II × 2 245 2.91 GHz with 1.75GB RAM and Matlab software (Mathwork, Natick, Massachusetts, US). The structure of the proposed inference model under AMI is shown in Fig. 7*c*. Two case studies, including 'NTL detection' and 'power blackout event', were conducted to demonstrate the effectiveness of the proposed model. The simulation results are described in detail as follows.

4.1 Feasibility tests for NTL detection

For the given related parameters in Table 1, the probability functions of three events can be expressed as individual payoffs using (11)–(13), and its conflicting probability functions are N', F', and B'. For multiple events identification with three agents in a game, the joint payoffs of the game are (s_1, s_4), (s_5, s_8), and (s_9, s_{12}), as shown in Fig. 8. The equilibrium points can directly be determined using the plot method and inequalities, represented by 'black circle' symbols. With setting the equilibrium points, $\Phi_1^* = \Phi_2^* = 1.35$ and $\Phi_3^* = 7.20$, the evolutionary dynamics of payoff profiles from N to F, N to B, and F to B can be expressed by the cooperative behaviours. According to these critical points, we have the following inferences with the constraint conditions to make decisions

$$\begin{cases} s_1 > s_4, & s_2 > s_4 \text{ for } N \text{ event} \\ s_1 < s_4, & (s_1 + 2 \times s_2) < (s_3 + 2 \times s_4) \text{ for } F \text{ event} \end{cases}$$

$$\begin{cases} s_5 > s_8, & s_5 > s_7 \text{ for } N \text{ event} \\ s_5 < s_8, & (s_5 + 2 \times s_6) < (s_7 + 2 \times s_8) \text{ for } B \text{ event} \end{cases}$$

$$\begin{cases} s_9 > s_{12}, & s_{10} > s_{12} \text{ for } F \text{ event} \\ s_9 < s_{12}, & (s_9 + 2 \times s_{10}) < (s_{11} + 2 \times s_{12}) \text{ for } B \text{ event} \end{cases}$$

The above mentioned joint payoff profiles are shown in Fig. 8.

Under an AMI environment, power utilities can monitor customers' load usages at the PCC in a micro-distribution system. Then, MDM performs validation, estimation, and editing tasks to identify real powers and blackout events, as shown in Fig. 7*a*. For example, Fig. 7*b* shows the five electrical customers' daily load profile, based on average load consumption during one working week. For load management, AMI provides bidirectional communications to the intelligent electric meters and the MDM system, which can also provide daily usage profile and meter-reading usage data in the metering point. Fig. 9*a* shows the first customer's profiled usages during three working days. It is found the customer has fraudulent activities between 7:00 (a.m.) and 13:00 (p.m.) on the second day, related testing data as shown in Table 2. With the profiled usage, $P_{1,\text{pro}}$, and the real-time measurement usage, $P_{1,\text{mea}}$, the ΔP_1 were computed using (1) as the durations of load changes. When decision $\Delta P_1 < -0.025$, the

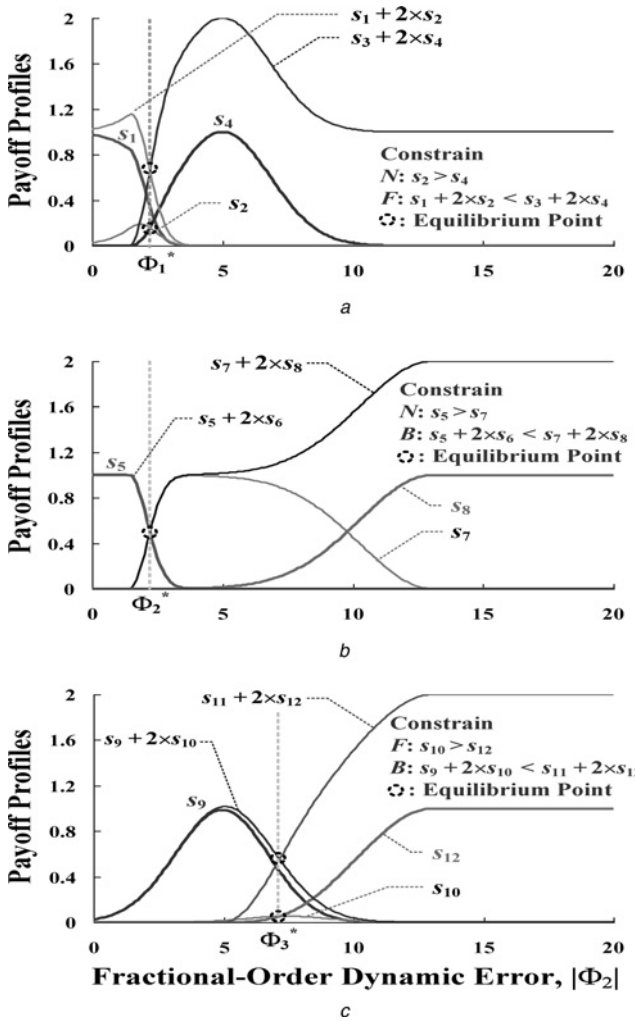

Fig. 8 *Multiple events identification with three agents in a game*

a Payoff profiles for separating normal condition (N) from fraud event (F)
b Payoff profiles for separating N from B
c Payoff profiles for separating F from B

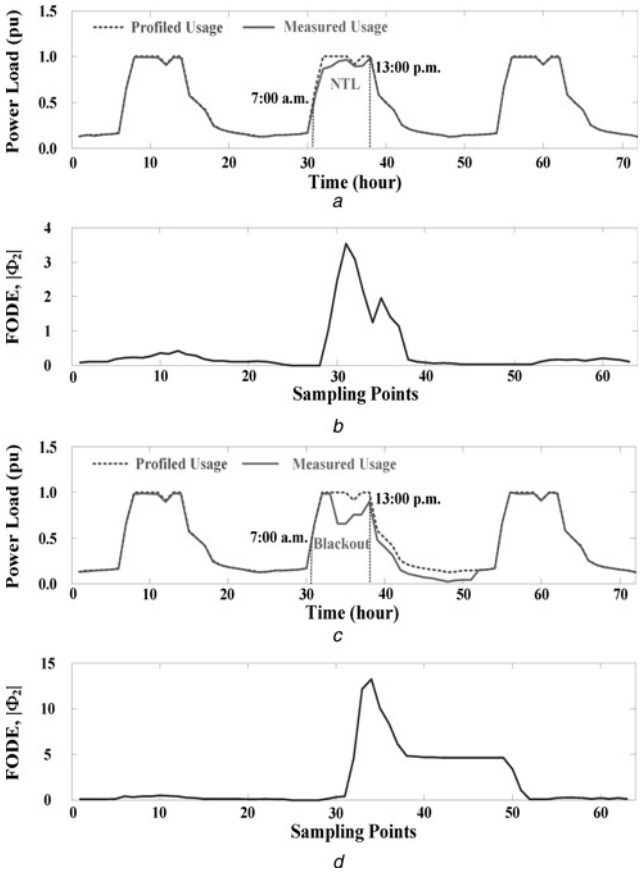

Fig. 9 *First customer's profiled usages during three working days*

a Simulation data for fraudulent activity (7:00 a.m.–13:00 p.m.)
b FODEs for fraudulent activity
c Simulation data for blackout event (7:00 a.m.–13:00 p.m.)
d FODEs for blackout event

Table 2 Simulation results for profiled usage, real-time measurement usage, and fraudulent activity detection

Time, t (a.m.)	$P_{1,pro}(t)$ pu	$P_{1,\ mea}(t)$ pu	ΔP	FODE $\lvert\Phi_2\rvert$	CG based Inference Mechanism								AI method	
					s_1	s_2	s_3	s_4	s_9	s_{10}	s_{11}	s_{12}	ANN	SVM
7:00	0.98	0.90	0.08	1.933	0.006	0.002	0.747	0.245	0.247	0.000	0.753	0.000	[0.45,0.54,0]	[0,1,0]
8:00	0.99	0.86	0.13	3.373	0.000	0.000	0.326	0.674	0.673	0.001	0.324	0.000	[0, 1, 0]	[0,1,0]
9:00	0.99	0.88	0.11	3.361	0.000	0.000	0.330	0.671	0.669	0.001	0.328	0.000	[0, 1, 0]	[0,1,0]
10:00	0.99	0.94	0.05	2.377	0.000	0.000	0.641	0.359	0.359	0.000	0.640	0.000	[0.01,0.99,0]	[0,1,0]
11:00	0.99	0.95	0.04	1.792	0.022	0.006	0.761	0.210	0.216	0.000	0.783	0.000	[0.70,0.29,0]	[0,1,0]
12:00	0.99	0.88	0.11	2.590	0.000	0.000	0.579	0.421	0.421	0.000	0.578	0.000	[0.28,0.72,0]	[0,1,0]
13:00	0.95	0.85	0.10	2.687	0.000	0.000	0.549	0.451	0.450	0.000	0.548	0.000	[0.25,0.75,0]	[0,1,0]

customer had overload, and decision $\Delta P_1 > 0$, the CGs based inference mechanism acted to perform the detection tasks. Therefore, we identified illegal events in the dropped changes of load usages, including $+0.025 \leq \Delta P_1 < +\ 0.050$ for '*likely F events*', and $+0.050 < \Delta P_1 < +\ 0.200$ for 'serious F events'. For example, timing measurements at 9:00 (a.m.), $\Delta P_1 = 0.11$, FODE $= |\Phi_2(\Delta \boldsymbol{P}_1)| = 3.361$, as seen in Fig. 9*b*, and index $S^- = S_1[s_1 = 0.000] \times (0.999)^4 = 0.000$ using the (17), the inference results are detailed according to the following procedure:

Step 1: for the given related testing data in Table 2, the probabilities (N, F, and B) against the load changes, ΔP_1, can be calculated using (11) to (13), and the conflicting probabilities are $N' = (1 - N)$, $F' = (1 - F)$, and $B' = (1 - B)$.
Step 2: overall payoff profiles, s_1 to s_8, can be calculated using (14), as seen in Table 2. As inference results, $(s_1,\ s_4) = (0.000,\ 0.671)$, $(s_5,\ s_8) = (0.000,\ 0.002)$, and $(s_9,\ s_{12}) = (0.669,\ 0.000)$, thus payoffs, s_5 to s_8, can be ignored.
Step 3: find the maximum payoff using (16), $S_2^+ = 0.671$, satisfying the constraint conditions:

- $s_1 < s_4$ and $s_1 + (2 \times s_2) = 0.000 < s_3 + (2 \times s_4) = 1.672$,
- $s_9 > s_{12}$ and $s_{10} = 0.002 > s_{12} = 0.000$,

where $m = 2$ for 'F event', as seen the payoff profiles in Figs. 8*a* and *c*. It takes < 0.10 s (average CPU time) to complete the FODE computations and CG based inference at each detection procedure, and then accurate detection results are achieved, as shown in Table 2. This confirms the proposed inference model is a promising method for 'fraudulent activity detection' in real time applications.

4.2 Feasibility tests for power blackout detection

Assuming the first electrical customer has five loads, L1: 1.5MW, L2: 1.2MW, L3: 0.8MW, L4: 1.2MW, and L5: 1.1MW. These five loads had heavy loads from 7:00(a.m.) and 13:00(a.m.) under normal operation. Let two electric equipment faults occur at L2# and L3#, then the protection relays acted to trip circuit breakers CB6 and CB7 (seen in Fig. 7*a*) to isolate the faulty equipment. The load usage dropped to 0.65pu at 9:00 (a.m.) on the second day, as shown in Fig. 9*c*. For the given testing data in Table 3, the changes in load usage were 0.01 pu and 0.34 pu during heavy load and power blackout, respectively. When the logic judgment, $\Delta P_1 > 0$, the FODEs, $|\Phi_2(\Delta P_1)|$, were computed using (10), as shown in Fig. 9*d*. The index, $S^- = (1.000)^2 \times 0.999 \times 0.988 \times 0.969 = 0.958$, pointed out the micro-distribution system operating under normal conditions, and then $S^- = 0.000$ indicated a '*blackout event* (B)' occurrence. For example, timing measurements at 10:00 (a.m), $\Delta P_1 = 0.34$ pu and $|\Phi_2(\Delta P_1)| = 14.09$, the CGs based inference mechanism also acted to perform the detection task, as seen the payoff profiles in Figs. 8*b* and 8*c*. Find the maximum payoff using (16), $S_3^+ = 0.934$, where $m = 3$ for '*B event*', satisfying the constraint conditions:

- $s_5 < s_8$ and $s_5 + (2 \times s_6) = 0.000 < s_7 + (2 \times s_8) = 1.868$,
- $s_9 < s_{12}$ and $s_9 + (2 \times s_{10}) = 0.000 < s_{11} + (2 \times s_{12}) = 1.934$,

After faulty equipment clearance, and load L3# can be repaired, confirming the proposed inference model can also detect the 'blackout events' from 14:00 (p.m.) to 24:00 (p.m.). Overall loads were energised on the third day. Then MDM system obtained the information of operation statuses and addressed the blackout event in the micro-distribution system.

4.3 Discussion

Compared with previous studies [1, 2, 8–14], traditional feature extraction methods with time-domain features or time-frequency features, such as historical consumption data, frequency spectra, and wavelet based features, have been used to identify differences between the profiled usages and meter reading usages. Then those combined classification methods, such as ANNs and SVMs, carried out pattern recognition or classification tasks, including 'likely' or 'serious' fraudulent events, but without detecting power blackout events in a local micro-distribution system. However, the average training accuracy reaches only 80 and 70% using ANN and SVM methods, respectively [2, 12].

In this study, fractional-order features were used to quantify the relationship between the FODEs, $\Phi_2|$, and the changes in load usages, $|\Delta P$. ANN and SVM methods are also applied in this research. Multi-layer networks with two nodes (ΔP and $\Phi_2|$) in the input layer, three nodes (N, F, and B with encoding in binary values) in the output layer, 110 hidden nodes for ANN method and three hidden nodes for SVM method are applied in continuous modelling systems with automatic network parameters and target adjustment. The least mean square (LMS) algorithm, gradient descent method, and optimisation method were used to find the optimum parameters to arrive at good detection accuracy using

Table 3 Simulation results for profiled usage, real-time measurement usage, and power blackout detection

Time, t (a.m.)	$P_{1,pro}(t)$ pu	$P_{1,\ mea}(t)$ pu	ΔP	FODE $\lvert\Phi_2\rvert$	CG based Inference Mechanism								AI Method	
					s_5	s_6	s_7	s_8	s_9	s_{10}	s_{11}	s_{12}	ANN	SVM
7:00	0.98	0.97	0.01	0.42	0.999	0.000	0.000	0.000	0.044	0.000	0.956	0.000	[0.84,0.16,0]	[1,0,0]
8:00	0.99	0.98	0.01	0.42	0.999	0.000	0.000	0.000	0.044	0.000	0.956	0.000	[0.84,0.16,0]	[1,0,0]
9:00	0.99	0.98	0.01	0.42	0.999	0.000	0.000	0.000	0.044	0.000	0.956	0.000	[0.84,0.16,0]	[1,0,0]
10:00	0.99	0.65	0.34	14.09	0.000	0.000	0.000	0.934	0.000	0.000	0.066	0.934	[0, 0, 1]	[0,0,1]
11:00	0.99	0.65	0.34	14.09	0.000	0.000	0.000	0.934	0.000	0.000	0.066	0.934	[0, 0, 1]	[0,0,1]
12:00	0.99	0.75	0.24	10.78	0.000	0.000	0.000	0.715	0.002	0.005	0.283	0.709	[0, 0, 1]	[0,0,1]
13:00	0.95	0.71	0.24	10.78	0.000	0.000	0.000	0.715	0.002	0.005	0.283	0.709	[0, 0, 1]	[0,0,1]

Table 4 Comparison of performances between the proposed model and other methods

Task	Method		
	CG	ANN	SVM
feature extraction	FODE $\|\Phi_2\|$	ΔP and FODE $\|\Phi_2\|$	ΔP and FODE $\|\Phi_2\|$
network architecture	matrix forms	multi-layer network I-H-O: 2-110-3	multi-layer network I-H-O: 2-3-3
training data	no	yes, major 110	yes, major 110
inference/learning algorithm	probability functions and inference formulations	• LMS algorithm • gradient descent method • optimisation method	
parameter assignment	yes minor	yes moderate	yes major
adjustable parameter	no	yes	yes
iteration training	no	yes	yes
convergent condition	no	yes	yes
testing data	100	100	100
accuracy	100%	90%	96%

Note: multi-layer network: input nodes (I)-hidden nodes (H)-output nodes (O)

training data, and convergent conditions were used to stop the iterative numerical computing. For the given 100 testing data, their detection accuracies are 90 and 96%, respectively. Some inference failures occurred in separating 'likely F events' from 'N events'. However, as seen in Table 4, learning performance relies on the choices of network parameter assignment, iteration computing, convergent conditions, and a large amount of training data.

The multi-layer networks provide promising solutions and high accuracies to perform the NTL and power blackout detection. With the increasing training data, network parameters' improvement was obtained by increasing the number of iteration computations using the optimisation methods. However, their algorithms are difficult implement in hardware devices, such as an embedded system or a microprocessor. The adjustable mechanism was suitable implemented and verified in a PC based detection model. The CG based model has matrix form presentations, fundamental mathematic operations, and logic composite operations to express the less parameterised decision reasoning. The equilibrium points are defined as a critical point to identify a certain event in Game I and Game II. Payoffs, s_1 against s_4, s_5 against s_8, and s_9 against s_{12}, have inverse behaviours for describing strategy combinations, (C, C) and (D, D). One's payoff is always greater than another payoff, and 100% accuracy can also be guaranteed to separate the fraudulent or blackout events from normal conditions with the specific constraint conditions. Its inference mechanism requires no assignment of an objective function, no iteration computing to update parameters, and no convergent conditions to terminate the algorithm. Therefore, CG based model can overcome the complexity of adjustable mechanism designs, such as ANN and SVM methods. It uses a straight-forward mathematical computation to produce inference results for real-time applications. The multiple agents have a joint payoff to sensitively detect any premonitory disturbance at each sampling stage, as the index, S^{-}, quickly dropped in the local micro-distribution system. The testing results also show promising solutions for NTL and power blackout detection, as shown in Tables 2–4.

5 Conclusion

Under the AMI technique, FODE formulations and multiple CGs have been employed to detect NTLs and power blackout events in a medium-scale micro-distribution system. FODE formulation was designed as the feature extractor and was easy to determine the specific parameters. It was used to quantify the relationship between the FODEs and the changes in load usages. The detection procedure was formulated as multiple agents in cooperation behaviours to solve the automatic inference tasks. The CGs based inference model provided a decision-making mechanism without iteration computation and updating parameters. The performances and simulation results showed greater effectiveness than multi-layer networks, such as ANN and SVM methods.

The growing number of micro-distribution systems has gradually led to challenges in energy, load, and billing management. An AMI provides an information connection between consumers and system operators, which is (i) has synchronised voltage, current, real power measuring capability, (ii) data collection, (iii) two-way communication capability to monitor the operating states in real-time, including residential and industrial consumers. System operators are able to refine the utility operating and process management tasks based on AMI. MDM system with automated software system performs long-term data collection, data storage, and outage managements, and then validates and processes it before this information is available to the billing system. Under the AMI workspace, the embedded system can be applied to design the proposed detection model in a short design cycle, including (i) connectivity information from the metering system; (ii) built-in digital signal processing; (iii) inference algorithm implement in a programmable processor. In contrast with multi-layer networks, it can be easily designed for integrating into an intelligent electric meter. The proposed inference model can also be further embedded in existing AMI/AGI workspace without the need of extra devices. For energy management applications, the CG based inference mechanism can both identify < 20% irregular usages during normal demand operations and blackout events within a few hours in a micro-distribution system.

6 Acknowledgment

This work was supported in part by the Ministry of Science and Technology, Taiwan, under contract number: MOST 103-2221-E-244-009 and MOST 104-2221-E-244-010, duration: 1 August 2014–31 July 2016.

7 References

1 Nizar, A.H., Dong, Z.Y., Wang, Y.: 'Power utility nontechnical loss analysis with extreme learning machine model', *IEEE Trans. Power Syst.*, 2008, **23**, (3), pp. 946–955

2 Nagi, J., Yap, K.S., Tiong, S.K., *et al.*: 'Non-technical loss detection for metered customers in power utility using support vector machines', *IEEE Trans. Power Deliv.*, 2010, **25**, (2), pp. 1162–1171

3 Nizar, A.H., Dong, Z.Y., Zhao, J.H.: 'Load profiling and data mining techniques in electricity deregulated market'. IEEE Power Engineering Society General Meeting, 2006, vol. 2, pp. 7–9

4 Mohsenian-Rad, A.-H., Wong, V.W.S., Jatskevich, J., *et al.*: 'Autonomous demand-side management based on game-theoretic energy consumption scheduling for the future smart grid', *IEEE Trans. Smart Grid*, 2010, **1**, (3), pp. 320–331

5 Navani, J.P., Sharma, N.K., Sapra, S.: 'Technical and non-technical losses in power system and its economic consequence in Indian economy', *Int. J. Electron. Comput. Sci. Eng.*, 2012, **1**, (2), pp. 757–761
6 Das, S., Ohba, Y., Kanda, M., *et al.*: 'A key management framework for AMI networks in smart grid', *IEEE Commun. Mag.*, 2012, **50**, (8), pp. 30–37
7 Sakis Meliopoulos, A.P., Cokkinides, G., Huang, R., *et al.*: 'Smart grid technologies for autonomous operation and control', *IEEE Trans. Smart Grid*, 2011, **2**, (1), pp. 1–10
8 Lin, C.-H., Chen, S.-J., Kuo, C.-L., *et al.*: 'Non-cooperative game model applied to an advanced metering infrastructure for non-technical loss screening in micro-distribution systems', *IEEE Power Eng. Lett., Smart Grid*, 2014, **5**, (5), pp. 2648–2649
9 Kim, S.I., Kim, H.S., Joo, Y.J., *et al.*: 'Power usage pattern and consumption separation method by load devices based on remote metering system's load profile data'. 2011 Int. Conf. on Control, Automation and Systems, 26–29 October 2011, pp. 1669–1671
10 Gerbec, D., Gasperic, S., Smon, I., *et al.*: 'Allocation of the load profiles to consumers using probabilistic neural networks', *IEEE Trans. Power Syst.*, 2005, **20**, (2), pp. 548–555
11 Rong Jiang, H.T., Lachsz, A., Jeffrey, M.: 'Wavelet based feature extraction and multiple classifier for electricity fraud detection'. 2002 Transmission and Distribution Conf. and Exhibition, 2002, vol. 3, pp. 2251–2256
12 Nagi, J., Yap, K.S., Tiong, S.K., *et al.*: 'Improving SVM-based nontechnical loss detection in power utility using the Fuzzy inference system', *IEEE Trans. Power Deliv.*, 2011, **26**, (2), pp. 1284–1285
13 Leon, C., Biscarri, F., Monedero, I., *et al.*: 'Variability and trend-generalized rule induction model to NTL detection in power companies', *IEEE Trans. Power Syst.*, 2011, **26**, (4), pp. 1798–1807
14 Cardenas, A.A., Amin, S., Schwartz, G., *et al.*: 'A game theory model for electricity theft detection and privacy-aware control in AMI systems'. Allerton Conf., 2012, pp. 1830–1837
15 Power sector news, KSEB officers' association: 'Pilferage of electricity-issues and challenges', available at http://www.kseboa.org/news/Pilferage-of-electricity-issues-and-challenges.html
16 Kuo, C.-L.: 'Design of an adaptive Fuzzy sliding-mode controller for chaos synchronization', *Int. J. Nonlinear Sci. Numer. Simul.*, 2007, **8**, (4), pp. 631–636
17 Erjaee, G.H., Alnasr, M.: 'Phase synchronization in coupled Sprott chaotic systems presented by fractional differential equations', *Discret. Dyn. Nat. Soc.*, 2009, **20**, p. 10
18 Kuo, C.-L., Lin, C.-H., Yau, H.-T., *et al.*: 'Using self-synchronization error dynamics formulation based controller for maximum photovoltaic power tracking in micro-grid systems', *IEEE J. Emerging Sel. Top. Circuits Syst. Spec. Issue Fractional-Order Circuits Syst.*, 2013, **3**, (3), pp. 459–467
19 Lin, C.-H., Chen, S.-J., Chen, J.-L., *et al.*: 'Using Sprott chaos synchronization based voltage relays for fault protection in micro-distribution systems', *IEEE Trans. Power Deliv.*, 2013, **28**, (4), pp. 2093–2102
20 Tucker, A.W.: 'The mathematics of tucker: a sampler', *Two-Year Coll. Math. J.*, 1983, **14**, (3), pp. 228–232
21 Nowak, M.A.: 'Five rules for the evolution of cooperation', *Science*, 2006, **314**, (8), pp. 1560–1563
22 Cavdar, I.H.: 'A solution to remote detection of illegal electricity usage via power line communications'. 2004 Power Engineering Soceity General Meeting, 6–10 June 2004, vol. 1, pp. 896–900
23 Bat-Erdene, B., Nam, S.-Y., Kim, D.-H.: 'A novel remote detection method of illegal electricity usage based on smart resistance', *Future Inf. Technol. Commun. Comput. Inf. Sci.*, 2011, **185**, pp. 214–223
24 Pandey, V., Gill, S.S., Sharma, A.: 'Wireless electricity theft detection system using Zigbee technology', *Int. J. Recent Innov. Trends Comput. Commun.*, 2013, **1**, (4), pp. 364–367
25 Li, F., Qiao, W., Sun, H., *et al.*: 'Smart transmission grid: vision and framework', *IEEE Trans. Smart Grid*, 2010, **1**, (2), pp. 168–177
26 Advanced distribution infrastructure, GE's AMI and DMS integration solution, available at http://www.gepower.com/prod_serv/products/metering/en/going_ami_new.htm
27 Nash, J.: 'Non-cooperative games', *Ann. Math. Second Series*, 1951, **54**, (2), pp. 286–295
28 Kadane, J.B., Larkey, P.D.: 'Subjective probability and He theory of game', *Manage. Sci.*, 1982, **28**, (2), pp. 113–120
29 Garagic, D., Cruz, J.B.: 'An approach to Fuzzy non-cooperative games', *J. Optim. Theory Appl.*, 2003, **118**, (3), pp. 475–491